observed only for the most basic compound, $Fe(phen)_2(CN)_2$. The three organometallic compounds studied were shown to exhibit high stability in melts of all compositions. For $Fe(phen)_2(CN)_2$ dissolved in the strongly acidic melts, the position of the +2/+3 couple was shown to shift by ca. 0.80 V, indicating that electron density is strongly drawn away from the metal center. However, for $Cp_4Fe_4(CO)_4$, the potential of the 0/+ couple remains fixed over the entire range of acidity. This is in keeping with MO calculations, which show that the HOMO of $Cp_4Fe_4(CO)_4$ is localized on the metal framework. This versatile room-temperature molten salt system is an excellent medium for studying the influence of Lewis acids on the redox reactions of organometallics.

Acknowledgment. We thank the Gas Research Institute (Grant 5082-260-0693) for financial support and Energy Research and Generation, Inc., for supplying the reticulated vitreous carbon. C.W. gratefully acknowledges helpful comments from Professors R. A. Osteryoung and John Wilkes concerning the nature of molten salts and from Dr. John G. Gaudiello concerning electrochemical techniques.

Contribution from the Department of Chemistry, University of Iowa, Iowa City, Iowa 52242

Synthesis and Magnetic Resonance Spectroscopy of Novel Phenolato-Bridged Manganese(III) and Iron(III)-Manganese(III) Porphyrin Complexes

Gregory M. Godziela, David Tilotta, and Harold M. Goff*

Received June 24, 1985

A novel manganese(III) porphyrin dimeric compound and an Fe(III)-Mn(III) heterodinuclear complex have been synthesized and structurally characterized by electronic and magnetic resonance spectroscopy. Metal derivatives of 5-(2-hydroxyphenyl)-10,15,20-tritolylporphyrin are susceptible to dimerization through formation of phenolato bridges. Monomeric (phenolato)-manganese(III) porphyrin complexes have also been prepared for the first time. Proton NMR spectral comparisons between the manganese(III) dimeric species and simple (phenolato)manganese(III) tetraphenylporphyrin provide justification for the phenolato-bridge hypothesis, allow for complete assignment of the porphyrin dimer NMR signals, and also permit comparison of spin-delocalization patterns for iron(III) and manganese(III) compounds. A spin-only magnetic moment of 5.0 μ_B and linear Curie law proton NMR plots indicate minimal antiferromagnetic coupling between the two manganese(III) centers of the dimeric species. The Fe(III)-Mn(III) heterodinuclear complex has been prepared in situ, but attempts to isolate the species free of homo dimers have been unsuccessful. Proton NMR and electron spin resonance spectra of solutions containing the mixed-metal dimer show new signals that are not seen in the spectra of the parent iron(III) and manganese(III) dimeric species.

Introduction

The coordination chemistry of manganese porphyrins is less well developed than that of corresponding biologically relevant iron porphyrins. More efficient porphyrin-manganese ion orbital overlap appears to weaken the interaction of axial ligands for the manganese center.[1] In comparison with iron(III) porphyrin analogues, manganese(III) porphyrins show lower affinity for addition of two axial ligands. Formation of the low-spin d^4 complex requires addition of two very strong field ligands such as imidazolate[2,3] or cyanide ions.[3,4] In noncoordinating organic solvents manganese(III) porphyrins are most likely to exist as neutral five-coordinate species bearing an anionic axial ligand. Coordinating solvents readily displace the anionic ligand to yield solvate complexes.

As is the case for other strong-field chelated manganese coordination compounds, the +3 oxidation state represents the air-stable form. Reduction to the +2 state[5] and oxidation to higher oxidation states are possible. Oxidation may be either porphyrin-centered[6] or metal-centered,[7] depending on the nature of the axial ligand(s). Synthetic manganese porphyrins have recently been shown to exhibit properties as oxidative catalysts that rival those of the iron analogues.[8] It thus appears important to improve our understanding of fundamental manganese porphyrin chemistry and to increase the diversity of available manganese prophyrin compounds.

Among manganese(III) porphyrins there are few examples of well-defined dimeric complexes. Polymeric imidazolato-bridged species have been characterized in the solid state.[2] The μ-oxo or μ-hydroxo dimer resulting from base hydrolysis[9] remains structurally undefined, although the further oxidized μ-oxo manganese(III)-manganese(IV) and manganese(IV)-manganese(IV) derivatives are unambiguously identified.[7] By comparison, numerous dimeric iron(III) porphyrin systems are known.

A dimeric iron(III) tetraarylporphyrin complex bridged by phenolato residues of the porphyrin has recently been prepared and structurally characterized both in solution and in the solid state.[10] The manganese(III) analogue is described here. This represents the first well-defined soluble dimeric manganese(III) porphyrin complex. In addition, it is shown that a novel mixed manganese(III)-iron(III) derivative is readily generated. Preparation of other mixed-metal complexes with the general structure I should also be possible.

Experimetal Section

Manganese Porphyrin Synthesis. The functionalized 5-(2-hydroxyphenyl)-10,15,20-tritolylporphyrin ($TTOHPH_2$) was prepared by condensation of 3 equiv of *p*-tolylaldehyde, 1 equiv of salicylaldehyde, and 4 equiv of pyrrole in a propionic acid reflux. The desired porphyrin was conveniently separated from other porphyrin products by sequential chromatography on alumina and silica gel columns.[10,11]

(1) Boucher, L. J. *Coord. Chem. Rev.* **1972**, *7*, 289-329.
(2) Landrum, J. T.; Hatano, K.; Scheidt, W. R.; Reed, C. A. *J. Am. Chem. Soc.* **1980**, *102*, 6729-6735.
(3) Hansen, A. P.; Goff, H. M. *Inorg. Chem.* **1984**, *23*, 4519-4525.
(4) Scheidt, W. R.; Lee, Y. J.; Luangdilok, W.; Haller, K. J.; Anzai, K.; Hatano, K. *Inorg. Chem.* **1983**, *22*, 1516-1522.
(5) Kadish, K. M.; Kelly, S. *Inorg. Chem.* **1979**, *18*, 2968-2971.
(6) Goff, H. M.; Phillippi, M. A.; Boersma, A. D.; Hansen, A. P. *Adv. Chem. Ser.* **1982**, *No. 201*, 357-376.
(7) (a) Schardt, B. C.; Hollander, F. J.; Hill, C. L. *J. Am. Chem. Soc.* **1982**, *104*, 3964-3972. (b) Smegal, J. A.; Hill, C. L. *Ibid.* **1983**, *105*, 2920-2922. (c) Smegal, J. A.; Schardt, B. C.; Hill, C. L. *Ibid.* **1983**, *105*, 3510-3515. (d) Camenzind, M. J.; Hollander, F. J.; Hill, C. L. *Inorg. Chem.* **1983**, *22*, 3776-3784.
(8) Smegal, J. A.; Hill, C. L. *J. Am. Chem. Soc.* **1983**, *105*, 3515-3521 and references therein.
(9) Fleischer, E. B.; Palmer, J. M.; Srivastava, T. S.; Chatterjee, A. *J. Am. Chem. Soc.* **1971**, *93*, 3162-3167.
(10) Goff, H. M.; Shimomura, E. T.; Lee, Y. J.; Scheidt, W. R. *Inorg. Chem.* **1984**, *23*, 315-321.

0020-1669/86/1325-2142$01.50/0

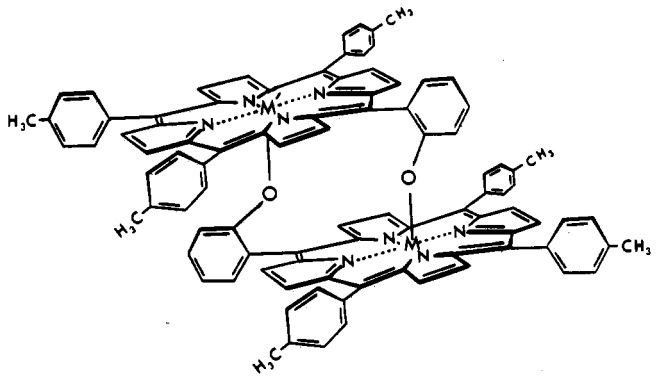

I

Manganese ion was incorporated into the macrocycle by addition of excess manganous acetate to a refluxing solution of the porphyrin in dimethylformamide. The manganese(III) porphyrin product (generated by air oxidation) was recovered from the cool dimethylformamide solution by addition of 2 volumes of aqueous saturated NaCl solution. The green solid was collected on a medium-porosity sintered-glass funnel, washed with methanol, and air-dried. Simultaneous purification and conversion to the bridged phenolato complex were effected by passage of a methylene chloride solution of the product through a column of basic alumina (Fisher A-941, Brockman Activity I). A 3% methanol–methylene chloride mixture was used to elute the green $((TTOP)Mn)_2$ compound. This eluate was filtered to remove any alumina particles and placed in a −20 °C freezer. After 2 days approximately 90% of the product was collected as a microcrystalline solid. The solid $((TTOP)Mn)_2$ was vacuum-dried at 60 °C for 24 h. Anal. Calcd: C, 77.9; H, 4.59; N, 7.73; Mn, 7.58. Found: C, 76.9; H, 4.41; N, 7.61; Mn, 7.43. The low experimental value for carbon exceeds analytical uncertainty and likely reflects retention of trace chlorinated solvent in the crystal lattice. Visible–UV spectral maxima in toluene (millimolar absorptivity values per manganese center in parentheses): 395 (46), 456 (58), 543 (6.9), 593 (5.9), 642 nm (7.5).

Monomeric axially ligated phenolato and *p*-methylphenolato complexes of manganese(III) tetratolylporphyrin ((TTP)Mn) were prepared by metathesis using the respective sodium phenolate salts. A small quantity (50 mg) of the chloromanganese(III) tetratolylporphyrin dissolved in 20 mL of methylene chloride was vigorously stirred for 8 h with 10 mL of an aqueous solution containing 0.25 g of NaOH and either 0.75 g of phenol or 0.90 g of *p*-cresol. Aqueous and organic layers were separated, and crystalline products were obtained by dropwise addition of heptane as the methylene chloride was removed under a nitrogen stream. Products were characterized by NMR (vide infra) and optical spectroscopy. Band positions in toluene solution: for $(TTP)Mn(OC_6H_5)$, 385, 450, 545, 590, 634 nm; for $(TTP)Mn(OC_6H_4(p\text{-}CH_3))$, 383, 450, 526, 625, 653 nm.

Mixed iron(III)–manganese(III) species were prepared on a small scale by dissolution of various quantities of $((TTOP)Fe)_2$ and $((TTOP)Mn)_2$ in a minimal volume of methylene chloride followed by treatment with gaseous HCl and immediate passage of all the material through a short basic alumina column with 3% methanol–methylene chloride as noted for the $((TTOP)Mn)_2$ derivative. Solvent was evaporated, and the mixture of dimeric complexes was vacuum-dried at 70 °C for 5 h.

Attempts to synthesize a pure mixed-metal dimer were also made. In these attempted preparations a mixture of the chlorometalloporphyrin compounds in methylene chloride was added to a short basic alumina column. A significant quantity of the iron porphyrin material was removed as the homo iron dimer by elution with methylene chloride. After iron dimer was removed, a solution of 3% methanol–methylene chloride was used to elute the remaining material. As the green manganese-containing porphyrin compounds began to move down the column, a brown compound was eluted off the column. A visible–UV spectrum of the brown material was identical with that of the iron dimer. The visible–UV spectrum of the first fraction of green material to elute from the column appeared to indicate a mixture of the iron and manganese dimers. It was later confirmed that this fraction contained a new mixed-metal dimer along with the homonuclear iron and manganese dimers.

Physical Measurements. Proton NMR spectra were recorded at 360 MHz on a Bruker WM-360 spectrometer. Solution magnetic susceptibility measurements were conducted by the Evans NMR method[12] through use of a 60-MHz spectrometer operating at 35 °C. Chloroform solutions 8 mM in $((TTOP)Mn)_2$ (on a monomeric concentration basis) contained 1% $(CH_3)_4Si$ as a reference substance. The reported magnetic moment for free-base tetraphenylporphyrin[13] and appropriate Pascal constants provided the basis for diamagnetic corrections. Density corrections for the sample and reference tubes were not necessary at this low concentration. Electron spin resonance measurements were made on a Varian E-104A spectrometer equipped with an Air Products LTD-3-110 Heli-Tran low-temperature system. The samples were run in 1:1 toluene–methylene chloride glasses containing porphyrin concentrations of 1.0–1.5 mM (on a monomer basis). Cyclic voltammetric measurements were made with a Princeton Applied Research 170 potentiostat and 175 Universal Programmer. Methylene chloride solutions contained 0.10 M tetrabutylammonium perchlorate and 1.5 mM metalloporphyrin. A platinum-bead working electrode was utilized, and potentials are referenced to the SCE.

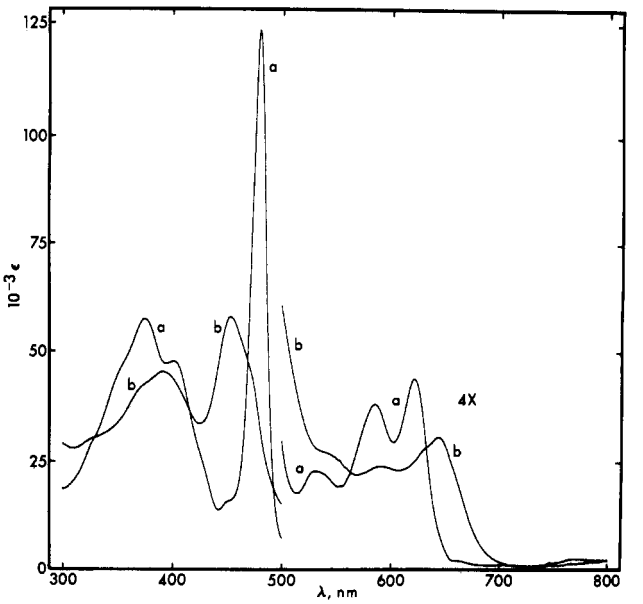

Figure 1. Electronic spectra of manganese(III) porphyrin complexes; (toluene solvent; 25 °C; 1.5×10^{-5} M total porphyrin): (a) (TTOP)MnCl; (b) $((TTOP)Mn)_2$.

Results

Dimeric Manganese(III) Complexes. Formation of the phenolato-bridged $((TTOP)Mn)_2$ species is indicated by several physical measurements. Optical spectra in Figure 1 show very significant differences for the chloro form and the basic alumina-hydrolyzed form. The spectrum of the presumably monomeric chloro complex in trace a matches that of the simple chloromanganese(III) tetraphenylporphyrin ((TPP)MnCl) derivative.[7c] Phenolato complexes of manganese(III) porphyrins have not been described previously, and thus no literature comparisons are available for the spectrum of $((TTOP)Mn)_2$ in trace b. However, optical spectra of the monomeric manganese(III) tetratolylporphyrin complexes containing phenolato and *p*-methylphenolato ligands are equivalent to the spectrum of $((TTOP)Mn)_2$. Shift of the 477-nm Soret band for the chloro complex to 456 nm for the phenolato adduct is consistent with empirical correlations for manganese(III) porphyrins that reveal blue shifts of this band for a more basic (i.e., phenolato) axial ligand.[1]

Proton NMR spectroscopy proves highly informative in terms of evaluation of the phenolato-bridge hypothesis. The spectrum for $((TTOP)Mn)_2$ and the far downfield and upfield regions of spectra for the monomeric phenolato species are shown in Figure 2. Assignments in Figure 2A are made on the basis of (1) those previously reported for simple manganese(III) tetraarylporphyrin complexes,[14] (2) the pattern of signals in Figure 2B,C, and (3) expected analogy in coordinated phenolato chemical shift pattern for iron(III) and manganese(III) tetraarylporphyrins. The pyrrole proton signal of symmetrical manganese(III) tetraarylporphyrins

(11) Little, R. G.; Anton, J. A.; Loach, P. A.; Ibers, J. A. *J. Heterocycl. Chem.* **1975**, *12*, 343–349.
(12) Evans, D. F. *J. Chem. Soc.* **1959**, 2003–2005.
(13) Eaton, S. S.; Eaton, G. R. *Inorg. Chem.* **1980**, *19*, 1095–1096.
(14) La Mar, G. N.; Walker, F. A. *J. Am. Chem. Soc.* **1975**, *97*, 5103–5107.

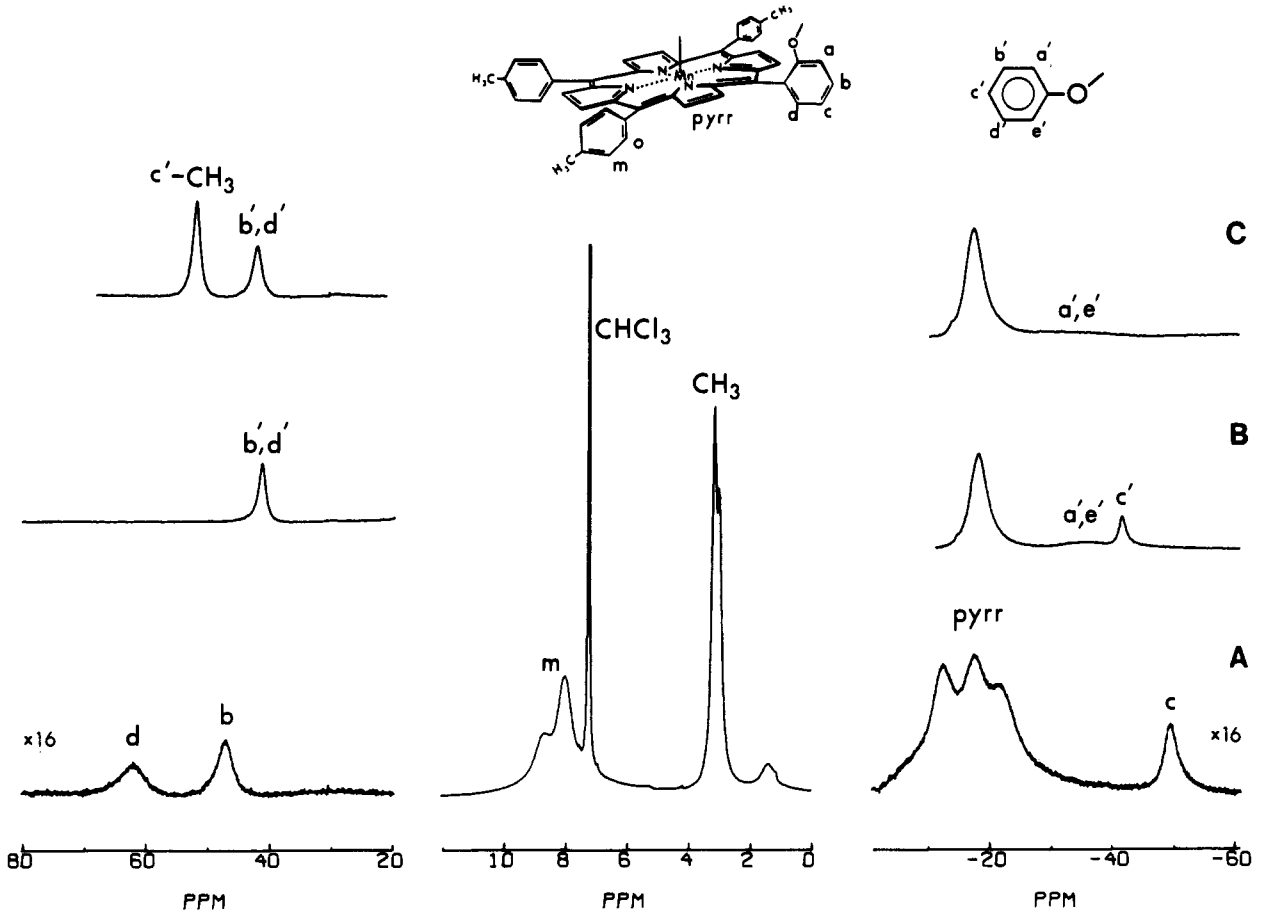

Figure 2. Proton NMR spectra of manganese(III) porphyrin complexes ($CDCl_3$ solvent; 25 °C; 0.01 M in total porphyrin; referenced to $(CH_3)_4Si$; 360-MHz operating frequency): (A) $((TTOP)Mn)_2$; (B) $(TTP)Mn(OC_6H_5)$; (C) $(TTP)Mn((OC_6H_4)(p\text{-}CH_3))$.

is seen in the −20 ppm region. Splitting of this signal is anticipated for $((TTOP)Mn)_2$, given the innate asymmetry of the functionalized porphyrin and enhanced asymmetry in the dimeric unit. The far upfield signal c has the intensity of a single proton and is unambiguously assigned through its absence in the spectrum of the *p*-methylphenolate complex. Peaks in the far downfield region of Figure 2A also have single-proton intensities, whereas signals representing two protons are seen in Figure 2B,C. Protons d and b in $((TTOP)Mn)_2$ are in the same relative positions with respect to the coordinated Mn(III) ion, and hence their chemical shift values are expected to be in the same direction and of the same magnitude. Proton a in the $((TTOP)Mn)_2$ spectrum is not detected but is presumably in a far upfield region much as is signal a′/e′ in the phenolato complex (Figure 2B). Methyl and phenyl meta signals for the three *p*-tolyl groups of $((TTOP)Mn)_2$ are located near the usual aliphatic and aromatic regions. In both cases these signals appear as two peaks with a 2:1 ratio of intensities. The 2:1 ratio of intensities is expected because there are two equivalent phenyl groups adjacent to and one phenyl group opposite the phenolato ring. The very broad tolyl ortho signals presumably lie under the tolyl meta resonances. Chemical shift values for all the assigned resonances are summarized in Table I.

Variable-temperature proton NMR spectra of $((TTOP)Mn)_2$ were recorded to evaluate Curie law behavior as revealed by plots in Figure 3 for selected signals. Curves are reasonably linear, but intercepts do not consistently match values expected for an analogous hypothetical diamagnetic complex. For example, porphyrin pyrrole signals in diamagnetic complexes are at 9.0 ppm, but the porphyrin pyrrole signal intercepts for $((TTOP)Mn)_2$ exhibit a downfield bias to 16.9 and 16.2 ppm. This behavior parallels the case for the monomeric (TPP)MnCl complex[14,15] and is thought to be due to a second-order Zeeman interaction. The coordinated phenolato signals likewise exhibit intercept values well outside the aromatic region. Linearity in plots over the temperature range available for $CDCl_3$ solvent indicates that antiferromagnetic coupling between metal centers must be relatively small. This conclusion is also supported by measurement of an essentially spin-only ambient-temperature magnetic moment of 5.0 ± 0.2 μ_B per manganese(III) center. Small antiferromagnetic coupling cannot be ruled out, however, and could account for deviations in Curie plot intercepts.

Table I. Proton NMR Chemical Shift Values (ppm) for Phenolato-Bridged Metalloporphyrin Complexes[a]

	homo dimers		hetro dimer	
signal	$((TTOP)Mn)_2$	$((TTOP)Fe)_2$	(TTOP)Mn–	(TTOP)Fe–
pyrrole H	−12.5	83.1	−12.0	83.1
	−17.7	79.2	−17.4	79.0
	−21.8	76.0	−20.4	75.7
tolyl ortho H	*b*	8.9	*b*	*b*
tolyl meta H	8.7	12.49	8.7	11.78
	8.0	11.38	8.2	11.24
		10.80		10.77
		10.53		10.56
				9.65
CH_3	3.14	5.61	3.10	5.61
	3.00	5.27	3.00	5.27
phenolate[c]				
b, d	62.2	108.2	108.4	60.9
	47.4	97.3	95.4	47.3
c	−49.5	−113.2	−112.3	−48.2
a	*b*	−115	~−115	*b*

[a] $CDCl_3$ solvent; 25 °C; 0.01 M in total porphyrin; referenced to $(CH_3)_4Si$, chemical shift uncertainties ±0.2 ppm for broad peaks and ±0.04 ppm for signals reported to two decimal places. [b] Broad signal not detected due to overlap. [c] See Figure 2 for the assignments of these signals.

(15) Goff, H. M.; Hansen, A. P. *Inorg. Chem.* **1984**, *23*, 321–326.

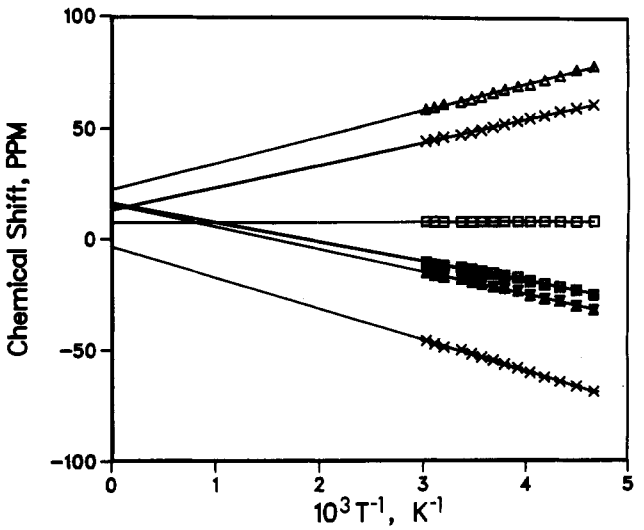

Figure 3. Curie law proton NMR plots for $((TTOP)Mn)_2$ ($CDCl_3$ solution; 0.01 M total porphyrin; referenced to $(CH_3)_4Si$). From bottom to top: upfield proton c; two pyrrole H signals; major tolyl meta proton; downfield phenolato proton b; downfield phenolato proton d.

Cyclic voltammetric measurements reveal reversible anodic waves at 1.21 and 1.60 V (SCE) for $((TTOP)Mn)_2$. Cathodic waves are complex and irreversible.

No electron spin resonance signals are seen at 77 or 5.8 K for a 1:1 toluene–methylene chloride glass of 1.5 mM $((TTOP)Mn)_2$ as is expected for an even-spin system.

Mixed Manganese–Iron Complexes. Hydrolysis of combined chloromanganese(III) and chloroiron(III) TTOP complexes on a basic alumina column serves to generate mixtures of $((TTOP)Mn)_2$, $((TTOP)Fe)_2$, and the new hetero dimer $(Mn(TTOP)_2Fe)$. Evidence for the expected mixed complex is found in high-resolution NMR spectra shown in Figure 4. Spectra are plotted for both homodimers as well as for mixtures containing 4:1 and 1:1 Mn:Fe analogues (spectra for additional metal ratios were also obtained but not included in Figure 4). Signals are apparent for homo dimers in both traces B and C of Figure 4. However, new signals (marked with arrows) are clearly evident in trace C at 95.4, 11.78, 11.24, 9.65, and −112.3 ppm. These signals are reasonably assigned to a Mn–Fe hetero dimer species. It is assumed that signals for the majority of protons in this new hetero dimer overlap with those of the respective homo dimers. Although new pyrrole signals are not resolved, changes in intensity and line width patterns occur in the pyrrole proton resonances of each metal complex due to the presence of overlapping signals of the hetero dimer. For example, the center 79.1-ppm $((TTOP)Fe)_2$ signal is considerably "broadened" by signal overlap in Figure 4B,C, for which appreciable amounts of the hetero dimer are present. Likewise, the −20 ppm region manganese porphyrin pyrrole signals are perturbed by partial formation of the hetero dimer.

The 95.4 ppm signal of the hetero dimer represents the b or d aromatic protons of a phenolato group that is a part of a manganese(III) porphyrin but is coordinated to an iron(III) center. The adjacent signal at 97.1 ppm is from the corresponding proton of the $((TTOP)Fe)_2$ dimer. If the hetero dimer was formed in a statistical manner, the intensities of 95.4 and 97.1 ppm signals in Figure 4C should be identical (one part homo dimer with two equivalent porphyrin centers and two parts of the hetero dimer). The homo dimer signal is clearly more intense in both traces B and C of Figure 4. Assuming that equilibrium conditions are achieved during the basic alumina hydrolysis step, the following equilibrium clearly lies to the left:

$$((TTOP)Fe)_2 + ((TTOP)Mn)_2 \rightleftharpoons Mn(TTOP)_2Fe$$

The electron spin resonance spectra at 5.8 K of both the homonuclear iron dimer and a sample containing mixed-metal dimer are shown in Figure 5. The iron dimer shows four signals located at g = 5.4, 3.4, 2.7, and 1.9. The ratio of the intensities of the g = 5.4 and 3.4 signals is variable, and we assume this is due to trace amounts of a monomeric five-coordinate iron porphyrin impurity. The sample containing the mixed-metal species shows signals at g = 6.7, 5.4, 3.4, and 1.9. A portion of the intensity of the signals at g = 5.4, 3.4, and 1.9 is due to the presence of iron dimeric and monomeric components in the sample. All of these signals broaden with increasing temperature until at 80 K only a broad, weak g = 6.7 signal can be seen. Although, the hetero dimer is formally an odd-spin system ($S = {}^5/_2$ and S = 2), absence of strong spin coupling and/or delocalization must

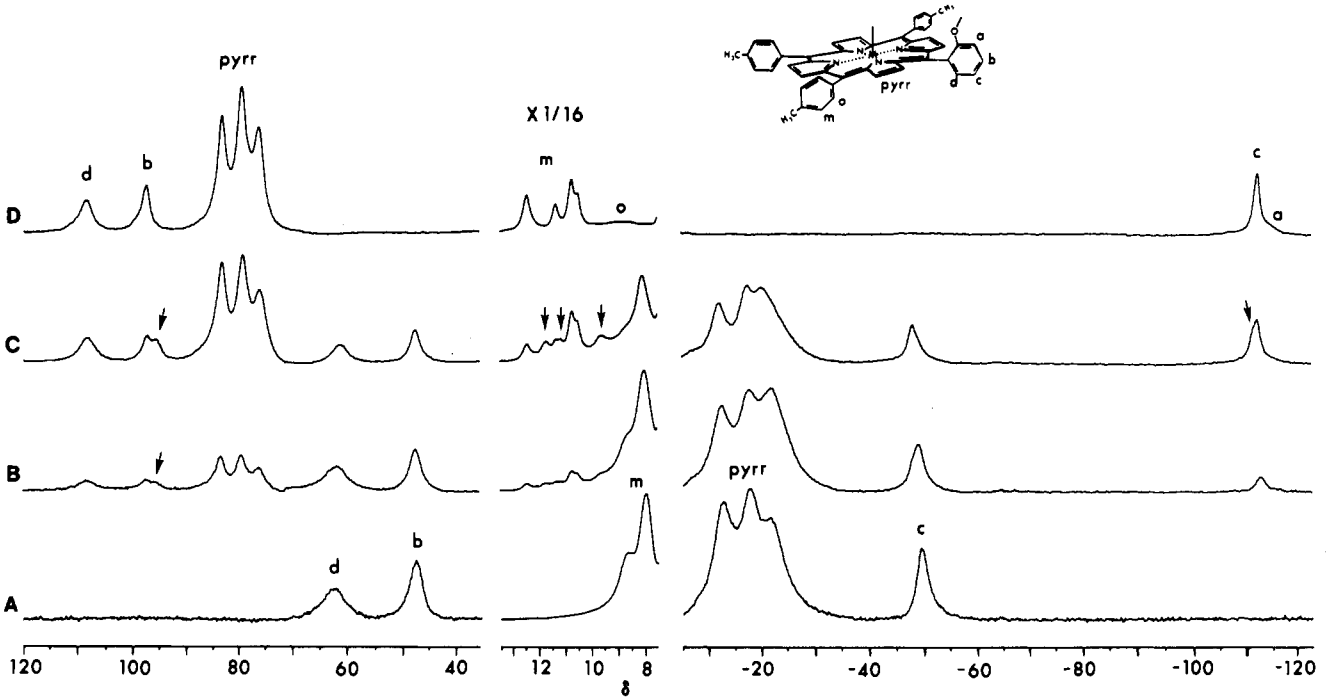

Figure 4. Proton NMR spectra of dimeric metalloporphyrin complexes ($CDCl_3$ solvent; 25 °C; 0.01 M in total porphyrin; referenced to $(CH_3)_4Si$; 360-MHz operating frequency): (A) $((TTOP)Mn)_2$; (B) 1:4 mixture of iron(III) and manganese(III) TTOP following base hydrolysis; (C) 1:1 mixture of iron(III) and manganese(III) TTOP following base hydrolysis; (D) $((TTOP)Fe)_2$. The arrows in traces B and C indicate new peaks that can be assigned to $Mn(TTOP)_2Fe$.

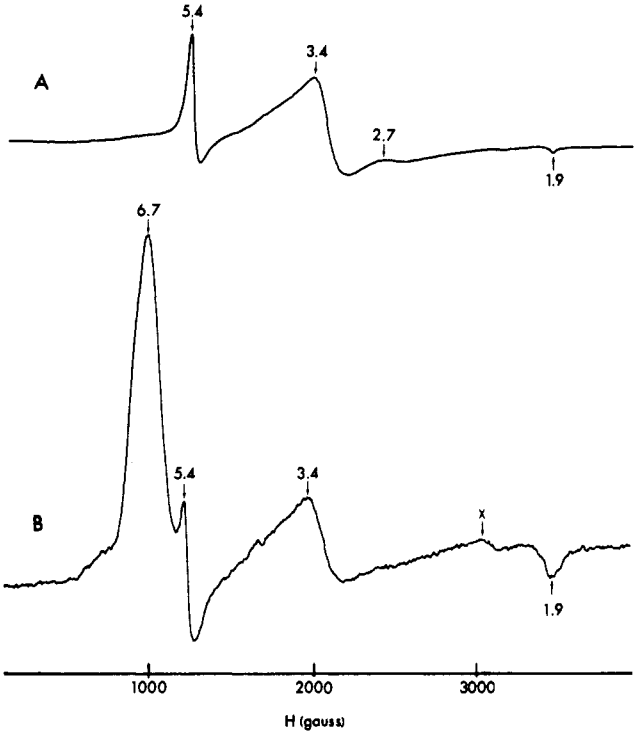

Figure 5. Electron spin resonance spectra of dimeric metalloporphyrin species (1:1 toluene–methylene chloride; 5.8 K): (A) $((TTOP)Fe)_2$; (B) mixture of $((TTOP)Fe)_2$, $((TTOP)Mn)_2$, and $Mn(TTOP)_2Fe$.

leave spin–spin relaxation between metal centers as the major contributor to broadening of the ESR signals at higher temperatures.

Optical spectra of solutions containing both the hetero dimer and homo dimers exhibit no new bands that could be assigned to the hetero dimer. It thus appears that band intensities are only a function of the total quantity of a particular metalloporphyrin in solution.

Discussion

Nuclear magnetic resonance spectroscopy of manganese(III) porphyrins has received only scant attention due to the large line widths evident for the high-spin d^4 ion. Deuterium resonances for coordinated pyridine residues have previously been identified in far downfield positions,[15] but no (phenolato)manganese(III) porphyrin complexes have previously been reported. Thus, it is of interest to compare spin density delocalization patterns for both iron(III) and manganese(III) porphyrins. An upfield-shifted pyrrole proton signal in manganese(III) tetraalkylporphyrins is well rationalized by the $(d_{xy})^1(d_{xz},d_{yz})^2,(d_{z^2})^1(d_{x^2-y^2})^0$ electronic configuration in which the π-symmetry $(d_{xz},d_{yz})^2$ unpaired spin is delocalized to the pyrrole β-carbon atoms. An additional unpaired electron in the strongly σ-interacting $d_{x^2-y^2}$ orbital of high-spin iron(III) porphyrins serves to induce large downfield pyrrole proton chemical shifts. Examination of Figure 4A,D reveals that chemical shift directions for coordinated phenolato ion are the same for both iron(III) and manganese(III) compounds. A singly occupied σ-symmetry d_{z^2} orbital is directed toward the phenolato oxygen atom in each case and must transfer appreciable spin density to the phenyl ring. Alternation in signs of chemical shifts around the phenyl ring is consistent with π-spin polarization of the phenolato aromatic ring. Transfer of manganese(III) spin density in this manner must be relatively less efficient than that of iron(III) as revealed by the approximate 50% attenuation of phenolato signal shifts in the manganese(III) derivatives.

Formation of the hetero Mn–Fe dimer under basic conditions is not surprising, but statistical distribution of dimeric species might have been anticipated. The metal discrimination involved in dimer formation likely reveals both thermodynamic differences in axial ligand bond formation and differences in the affinity of the porphyrins to the basic alumina column. The higher affinity of iron porphyrins for axial ligands and oxophilic character of the iron(III) center suggest that $((TTOP)Fe)_2$ is thermodynamically the most stable species among the three possible dimeric structures. Formation of the homo iron dimer upon addition of 3% MeOH–CH_2Cl_2 to the basic alumina column containing the hetero dimer indicates that all three dimeric species are in equilibrium. As $((TTOP)Fe)_2$ is produced, it is eluted down the column faster than the manganese-containing species and cannot be used to re-form the mixed-metal dimer. Hence, isolation of the pure Fe–Mn dimer by standard chromatographic methods is unlikely.

Generation of the mixed Mn–Fe porphyrin is rather facile, and in principle the $TTOP^{2-}$ ligand might be utilized to generate a large variety of homo and hetero dimetal complexes. Combinations of Cr(III), Mn(III), Fe(III), and Co(III) mixed species should be readily accessible. This general technique for preparation of mixed-metal complexes of defined geometry is thus offered for investigations of electron transfer and spin–spin interactions between metal centers and as a potential source of compounds for multielectron-redox catalysis.

Acknowledgment. Support from National Science Foundation Grant CHE 83-17451 is gratefully acknowledged. The Bruker WM-360 NMR spectrometer was purchased in part with National Science Foundation Grant CHE 82-01836.

Contribution from the Department of Chemistry, University of Queensland, Brisbane, Australia 4067

Cobalt(III) Complexes of L-Histidylglycylglycinate: Preparation, Characterization, and Conformation

Clifford J. Hawkins* and Jill Martin

Received October 7, 1985

The preparations of three cobalt(III) complexes of L-histidylglycylglycinate are reported. In one complex, $[Co(NH_3)(H_{-2}HisGG)]$, the peptide is coordinated as a quinquedentate chelate through the terminal NH_2, two deprotonated peptide nitrogens, the carboxylate, and the imidazole group. In another, $[Co(NH_3)_2(H_{-2}HisGG)]$, the carboxylate is replaced by a second NH_3. The third complex has properties consistent with the superoxo binuclear complex $NH_4[(H_{-2}HisGG)Co(O_2^-)Co(H_{-2}HisGG)]$. The structures of the first two complexes were derived from the complexes' electronic absorption, circular dichroism, and ^1H and ^{13}C NMR spectra. The coordinated imidazole's NH-1 has acid dissociation constants at 298 K of 10.73 ± 0.04 and 10.69 ± 0.04 for $[Co(NH_3)(H_{-2}HisGG)]$ and $[Co(NH_3)_2(H_{-2}HisGG)]$, respectively. In the diammine complex, the free carboxylate group has a pK_a value of 4.34 ± 0.04 at 298 K.

Introduction

This paper reports the first examples of N-terminal histidine peptides coordinating to a metal via the NH_2, the imidazole moiety, and two peptide-N^- donors. The complexes involve the coordination of L-histidylglycylglycinate to cobalt(III) with and without the terminal CO_2^- bound to the metal (Figure 1).

0020-1669/86/1325-2146$01.50/0